Journal of Ceramic Processing Research. Vol. 26, No. 6, pp. 1009~1023 (2025)
(Received 23 July 2025, Received in revised form 28 October 2025, Accepted 6 November 2025)
https://doi.org/10.36410/jcpr.2025.26.6.1009

J O U R N A L O F
Ceramic Processing Research

Synergistic effects and optimization of surface-modified borassus and madar fibers in hybrid epoxy composites with lotus seed powder filler

Shruti Gomkale[a], Abdulrahman Khamaj[b], Abdulelah M. Ali[c], Rajasekaran Saminathan[d], P Satishkumar[e,*], M. Naga Swapna Sri[f], Deepak Gupta[g] and Vijayakumar Sivasundar[h]

[a]*Assistant professor, Department of Applied Chemistry, Yeshwantrao Chavan College of Engineering, Nagpur, Maharashtra, India*
[b]*Industrial Engineering Department, College of Engineering and Computer Science, Jazan University, Saudi Arabia*
[c]*Industrial Engineering Department, College of Engineering and Computer Science, Jazan University, Saudi Arabia*
[d]*Mechanical Engineering Department, College of Engineering and Computer Science, Jazan University, Saudi Arabia*
[e]*Department of Mechanical Engineering, Rathinam Technical Campus, Coimbatore, Tamilnadu, India*
[f]*Department of Mechanical Engineering, Prasad V Potluri Siddhartha Institute of Technology, Vijayawada, Andhra Pradesh, India*
[g]*Department of Mechanical Engineering, Graphic Era Hill University, Dehradun-248002, Uttarakhand, India*
[h]*Department of Mechanical Engineering, Saveetha School of Engineering, SIMATS, Chennai 602105, Tamil Nadu, India*

The aim of this work is to enhance the mechanical properties of hybrid epoxy composites reinforced with Borassus fruit fibers (BFF) and Madar fibers (MF), fabricated by conventional hand layup technique. Composite formulations were created by adjusting fiber reinforcement levels (0–12 wt%) and integrating lotus seed shell powder (LSSP) as a filler (2–4 wt%), while adding benzoyl chloride surface treatment (BT) (0–6 wt%) enhanced the fiber–matrix interfacial bonding. This study examines the FTIR spectra of MF, BFF, and LSP subjected to 0%, 3%, and 6% BT. A comprehensive multi-criteria decision-making (MCDM) technique was utilized to determine the optimal composite structure, incorporating the CRITIC approach for objective weighting of mechanical performance characteristics with two sophisticated ranking algorithms — CODAS and MARCOS. The optimization results showed that, the composite consists of 12 wt% BFF, 12 wt% MF, 3 wt% BT, and 2 wt% LSSP, exhibited improved mechanical properties. Specifically, the composite achieved a tensile strength (TS) of 38.6 MPa, a flexural strength (FS) of 63.25 MPa, and an impact strength (IS) of 69.63 J/m. The enhanced fiber-matrix bonding resulting from surface modification and the synergistic effects of hybridization are the reasons for the improved performance. In addition, a sensitivity analysis was performed by altering the weights of the testing composite to determine their impact on the overall ranking. The hybrid optimization and experimentation indicate that ninth composites have superior mechanical properties relative to other fabricated composites.

Keywords: Mechanical properties, Flexural strength, Lotus seed shell powder, Optimization, CODAS, MARCOS.

Introduction

The growing environmental concerns and the non-biodegradability of synthetic fibers have intensified research on sustainable natural fiber-reinforced polymer composites. Natural fibers are suitable alternatives for lightweight structural applications due to their bio-degradability, renewability, and low density. Nevertheless, their mechanical performance was influenced by their hydrophilic nature, which restricts their compatibility with hydrophobic polymer matrices. Surface modification techniques like benzoyl chloride treatment enhanced the fiber–matrix bonding. The study explored the moisture absorption behavior of coconut fiber composites after chemical treatments (acetone, alkali, and benzoyl). Composites with 25 wt.% fiber content were tested at different immersion times (0–10 hrs). Benzoyl-treated fibers showed the least moisture uptake, indicating improved hydrophobicity. These results highlight the benefit of benzoylation for moisture-resistant natural fiber composites [1].

Short Borassus fiber-based composites were fabricated and tested for mechanical strength and water absorption at various water sources. Fibers were alkali-treated using 4 wt%, 8 wt%, and 12 wt% NaOH concentrations. Higher concentrations improved tensile, flexural, and impact strengths while reducing water uptake. SEM showed an increase in surface roughness, promoting better bonding with the matrix [2]. In rcent research across various fiber types, including Borassus fibers supports the global adoption of natural composites. The findings investigate the wider use of eco-friendly fibers in structural and functional applications [3]. This study extracted and characterized a new natural fiber from

*Corresponding author:
Tel : +91 9791927002
E-mail: sp.sathishkumar10@gmail.com

Nelumbo nucifera (lotus stem) through alkali treatment. Structural and thermal analysis showed a crystallinity index of 52.53% and thermal stability around 210 °C. Composite samples (L10–L20) were prepared with epoxy to evaluate mechanical strength. The L20 composite exhibited superior tensile and flexural properties, highlighting its potential for household applications [4]. The researchers investigated the epoxy composites using chemically and microwave-treated *madar* fibers with *Nelumbo nucifera* filler. Composite mats were fabricated and tested for mechanical, and viscoelastic properties. A 10 wt% NN filler provides the optimal performance and higher content reduced the mechanical strength [5]. The rhizome of *Nelumbo nucifera* was processed into powder and characterized for composite filler applications. XRD confirmed a crystallinity index of 57.7% and nanoscale crystallite size. These traits validate the suitability of the rhizomes as a sustainable polymer filler [6].

This study developed hybrid epoxy composites using 40% *Calotropis gigantea* (madar) fiber and bran nanofillers. Mechanical testing showed that increasing MF content improved tensile (20.8 MPa), flexural (24.1 MPa), and impact strength (23 J). However, bran filler enhanced the thermal stability up to 448 °C. SEM analysis revealed good fiber-matrix bonding and identified post-failure fracture modes [7]. The researchers studied how fiber length affects the TGA and DMA of madar fiber-reinforced epoxy composites. Samples with varying lengths were analyzed using TGA and DMA. Interfacial bonding between fiber and matrix influenced viscoelastic behavior under temperature variations. The study identified optimal fiber length for maximizing composite quality [8]. A hybridized composite of glass and madar fibers strengthened with porcelain particles in epoxy was developed using compression molding. Mechanical and DMA analyses confirmed the enhancement in strength, microstructural integrity, and viscoelasticity (4.2% increase) with improved thermal stability of upto 357 °C. The composite is suited for structural applications due to its robust properties. SEM analysis confirmed reduced fiber delamination and better internal structural integrity [9, 10].

Hybrid composites were made with five laminate using varying stacking sequences of jute, Madar, and Glass fibers (GJMJG, GMJMG, GJGJG, GMGMG). Mechanical testing showed that jute increased the strength while madar improved strain and toughness. Glass fibers as skin layers significantly boosted composite properties. SEM of fracture surfaces revealed good fiber-matrix compatibility [11]. Eco-friendly printed circuit boards (PCBs) were developed using banana (40%) and madar (20%) fibers in epoxy (40%) composites. The composite demonstrated excellent mechanical and electrical properties like tensile strength, dielectric constant, and peel strength. Low water absorption (3.54%) and stable signal integrity support its application as a sustainable PCB alternative [12]. A hybrid composite of madar and bamboo fibers was fabricated using hand layup for tensile testing. Experimental tensile results were validated through finite element analysis (FEA) in ANSYS. The FEA model successfully simulated tensile behavior, allowing prediction of strength for various ply angles. A regression equation was formulated for future design optimization [13]. Natural Borassus fruit fiber and synthetic cigarette butt fiber were used in vinyl ester matrix with 0–10% eggshell powder. Composites with 40 wt% Borassus fruit fiber, 40 wt% cigarette butt fiber and 5 wt% eggshell powder showed maximum tensile (53.62 MPa), flexural (38.67 MPa), and impact (37.78 J/m) strengths. Advanced characterization and CRITIC–EDAS approach identified as this composite was optimal. Sensitivity analysis verified robustness of the ranking [14].

A hybrid MCDM technique combining CRITIC and CODAS was developed to rank automotive brake friction composites reinforced with hemp, ramie, pineapple, banana, and Kevlar fibers at 5% and 10% loadings. It provides a more robust and discriminative ranking mechanism by considering both the Euclidean distance and the Taxicab (Manhattan) distance from the negative-ideal solution. While EDAS evaluates alternatives based only on positive and negative deviations from average performance, and WASPAS relies on weighted aggregation of normalized values, CODAS effectively captures multi-dimensional performance variations and minimizes ranking ambiguity in closely competitive alternatives. This dual-distance approach enhances decision reliability, particularly for complex datasets involving multiple correlated mechanical parameters, making CODAS more suitable for precise and stable optimization of hybrid composite properties. Key properties like coefficient of friction, wear, density, and environmental impact were criteria. The composite with 10 wt.% banana fiber was identified as optimal for balanced performance. Sensitivity and correlation analyses confirmed robustness of the ranking [15]. This study applied CRITIC and ranking methods (TOPSIS, SAW, MARCOS) to select the best natural fiber reinforcement for PA 66 polymer composites in light gun manufacturing. Banana fiber ranked highest due to its favorable mechanical properties, particularly Young's modulus (weight 0.180). Correlations between the methods were confirmed by Spearman coefficients. The approach aids material decision-making in defense applications [16]. The MARCOS method was implemented initially in textile fiber selection to rank 17 cotton lots by quality, using six fiber properties weighted by AHP. Lot C9 achieved the highest utility, while C7 ranked lowest. Results aligned well with previous methods and yarn tenacity rankings, showing robustness without rank reversals. The study highlights MARCOS as a flexible, accurate MCDM tool for textile industry decisions [17]. Several researchers have investigated the performance of epoxy based composites and optimized

the machining characteristics [31, 32].

Although extensive research has been conducted on individual natural fibers for composite reinforcement, limited studies have investigated the synergistic mechanical effects of combining BFF and MF in a hybrid epoxy matrix. Furthermore, the optimization of such hybrid composites incorporating eco-friendly fillers like LSSP, along with surface modification techniques such as BT, remains underexplored. Previous works lack a comprehensive multi-criteria optimization technique that balances multiple performance indices. This study uniquely addresses these gaps by integrating CRITIC-CODAS-MARCOS decision-making models to determine the optimal composite formulation. The novelty lies in the strategic hybridization of BFF and MF, surface functionalization through benzoylation, and the addition of LSSP to develop a high-performance, sustainable composite system with enhanced tensile, flexural, and impact properties. The LSSP content was limited to 4 wt% to maintain an optimal balance between filler dispersion and mechanical performance. Beyond this threshold, particle agglomeration and poor interfacial wetting tend to occur, leading to stress concentration sites and reduced composite strength. Hence, restricting LSSP to 4 wt% ensures uniform dispersion, effective stress transfer, and stable mechanical enhancement without compromising the composite's structural integrity or fabrication quality.

Experimental Methodology

Materials

Madar and Borassus fruit fibers is collected from various location in Coimbatore district, Tamilnadu, India, were chosen as the reinforcing material for this experiment. Lotus seed shell powder was purchased from Sri Balarama Chettiar Enterprises, Bhavani, Erode, Tamilnadu, India. The matrix composed of Epoxy LY556 and hardener HY951 in a 10:1 ratio was procured from Kovai Cheenu Enterprises in Coimbatore, Tamilnadu, India [18]. The hydrophilic properties were reduced by exposing the fibers to the chemical treatment using the benzoylation process (0–6 wt%). This surface treatment replaces the hydroxyl groups with benzoyl groups.

Preparation of hybrid fiber

Madar fibers are obtained by the collection of mature stems and submerging them in water for a duration of 3 weeks. At this stage, the pectin responsible for binding the fibers undergoes degradation. The softened outer layer was eliminated by employing a brush and the fiber were physically pulled out from the bark. Then after the fibers are washed in running water to remove any leftover pectin and dirt. The refined fibers were scattered to promote complete evaporation [19].

The fibers are extracted from the outer layer of the Borassus fruit and separated from the fruit through the retting process. Consequently, the filaments were removed after immersion in water to promote their disintegration. Initially, researchers extracted the pure fibers and subsequently dehydrated them for 48 hours. The impact of variance was reduced by extensively homogenizing the fibers following the extraction. Consequently, the unprocessed Borassus fruit fiber was obtained [20]. Fig. 1 illustrates the extraction method of fiber from the Madar plant and Borassus tree.

Fig. 1. Preparation of hybrid fibre.

Preparation of lotus seed shell powder

Lotus seed shells (*Nelumbo nucifera*) were manually separated from mature seeds, thoroughly rinsed with distilled water, and sun-dried for 2–3 days to remove surface moisture. Thereafter, the shells were oven-dried at 100 °C for 4 hours to achieve complete dehydration. The dried shells were then grounded using a high-speed grinder to produce a fine powder, which was passed through a 50-mesh stainless steel screen to ensure uniform particle size. The resulting Lotus Seed Shell Powder was stored in sealed zip-lock bags under dry conditions until further use. This biodegradable lignocellulosic filler

Fig. 2. a) Lotus seed b) Lotus seed shell powder.

was employed to improve the mechanical and interfacial properties of the composites [21]. Fig. 2 shows the lotus seed and the seed shell powder.

Surface treatment of natural fibers

A 6 wt% NaOH solution was employed to dissolve hemicellulose, pectin, oil, wax, and other impurities from MF and BFF during the initial stage. The hydrogen bonds is disrupted by the NaOH treatment, which was applied for three hours. Excess NaOH was removed from the treated fibers by rinsing them with distilled water and ethanol. In the subsequent stage, benzoyl chloride treatment was applied at a concentration of 3 and 6 wt% for a duration of 2 hours. The hydrophilic nature of the BFF and MF was reduced due to the replacement of hydroxyl (OH) groups with benzoyl groups during this surface treatment. The mixture of MF and BFF with the benzoyl chloride solution was filtered, rinsed with distilled water, and then dried using filter paper. Subsequently, the fibers were thoroughly rinsed with distilled water following immersion in ethanol for 1 hour to remove any residual benzoyl chloride [22]. The fibers were then dried in a hot air oven at 70 °C for 6 hours to eliminate moisture content. Finally, the fibers chopped to a length of 10 mm for the fabrication of composite laminates.

FTIR analysis

To identify the various functional groups present in both the untreated and alkali-treated specimens, FTIR analysis was performed. Each sample was mixed with 2 mg of potassium bromide (KBr) to prepare pellets for FTIR analysis [23]. The materials were then analyzed using an FTIR spectrometer (Bruker, ALPHA II). The instrument was set to collect the data at a wavenumber range of 4000–400 cm^{-1}, with 32 observations at an interval of 2 cm^{-1}.

Fabrication of composite

The integration of MF and BFF (hybrid fibers) with an epoxy resin matrix was varied from 0 to 12 wt% to produce composite prototypes. The hand lay-up technique was employed for the fabrication of the composites. MF and BFF reinforced epoxy hybrid composite specimens were manufactured using different LSSP particle compositions. The wax was initially applied to the mold, which served as a release agent, and had the dimensions of 300 × 250 × 3 mm. The epoxy resin and hardener were then mixed with 10:1 ratio according to the manufacturer's instructions. The hardener acts as a curing agent for anhydrous bases. After the epoxy and hardener was thoroughly mixed, the LSSP was incorporated into the epoxy matrix. To prevent agglomeration due to the chemical reaction, the epoxy-LSSP mixture was stirred at 1200 rpm for 5 minutes using a mechanical stirrer. The mold surface was then coated with epoxy resin. A random arrangement of

Fig. 3. Experimental process for the fabrication of composites.

hybrid fibers was placed into the mold, and the epoxy mixture was poured over it to form the base layers of the specimens. The composite was compressed using an additional steel plate, which was covered with plastic to prevent adhesion to the mold. The specimen was allowed to cure at ambient temperature for 24 hours. After curing, the composite is removed from the mold. The mold is subsequently cleaned in preparation for the next fabrication cycle, following as per ASTM standards. The weight percentage of each fiber were varied from 0 to 12 wt%. The amount of epoxy required to fill the mold was calculated based on the weight of the fibers and binder used for each sample. Fig. 2 illustrates the composite fabrication process.

Testing analysis of Composite

Tensile strength

The tensile characteristics of the fabricated composites specimens were assessed as per ASTM D638-17 using FIE - UNITEK-94100 Universal testing machine (UTM) with a maximum load capacity of 400 kN (Fig. 3). Dog-bone-shaped specimens, measuring 57 mm in gauge length and 165 × 19 × 3 mm in overall dimensions, were prepared for testing. All samples were securely clamped in the machine and subjected to a constant load at a crosshead speed of 2 mm/min until failure occurred.

Flexural Testing

Flexural properties were assessed following ASTM D790-17 using the three-point bending setup of the universal testing machine (UTM). The specimens used for this test measured 125 × 12.7 × 3.2 mm. Each specimen was subjected to a load until fracture, at a constant crosshead speed of 2 mm/min. This evaluation provided insights into the bending strength and stiffness of the composite samples under flexural stress.

Impact Testing

In accordance with ASTM D256-10, the impact strength of the composites was assessed using an Izod

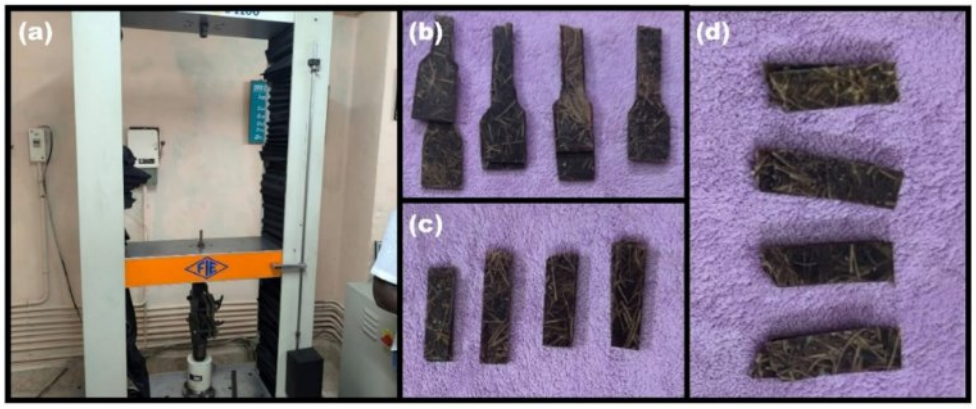

Fig. 4. An illustration of (a) Universal testing machine (b)Tensile test specimens (c) Flexural test specimens (d) Impact test specimens after testing.

impact testing machine. Rectangular specimens with dimensions of 127 × 12.7 × 3 mm were used for this purpose. The energy absorbed by the sample during a sudden impact was measured in the test, which indicates the resistance of the materials to dynamic loading and toughness.

Enhancement of fabricated composites by the Taguchi methodology:

Taguchi optimization technique is employed to evaluate a wide range of data by considering various factors and levels. It is used to assess the impact of input variables on different applications. Mechanical parameters, including tensile strength (TS), flexural strength (FS), and impact strength (IS), were evaluated for the BFF/MF composites. Both the fibers were treated with benzoyl chloride, and their weight percentages served as input variables. The Taguchi technique calculated the signal-to-noise (S/N) ratio to identify optimal factors by minimizing noise. Eq. (1) was employed to determine the optimal S/N ratio for the mechanical properties after all configurations were evaluated based on quality characteristics. The statistical software Minitab 20 was used for optimization. The mechanical strength of polymer-based composites is influenced by the bonding strength at the fiber/matrix interface. Four variables were used: MF (0–12 wt%), BFF (0–12 wt%), LSSP (2–4 wt%), and BT (0–6 wt%). To determine the optimal combination, an L9 orthogonal array was implemented. The L9 orthogonal array was selected in the Taguchi design to maintain a balance between experimental efficiency and statistical reliability. Since the study involved a limited number of key factors (fiber content, filler content, and surface treatment) at three levels each, the L9 array effectively captured their main effects with minimal experiments. Larger arrays like L16 or L27 are typically used when higher-order interactions or additional parameters are investigated; however, they significantly increase the number of trials, time, and material costs. As preliminary trials showed negligible higher-order interactions, the L9 array was sufficient to achieve accurate optimization with reduced experimental complexity and resource consumption.

$$\text{S/N Ratio} = -10\log_{10}\left[\frac{1}{n}\sum_{i=1}^{n}(1/y_i^2)\right] \quad (1)$$

The number of results is denoted by "n," while the results for the specific combinations are denoted by "y_i."

Multi response optimization

An integrated multi-criteria decision-making (MCDM) technique was implemented to obtain the optimal composite configuration based on mechanical performance. This framework employed the Criteria Importance Through Intercriteria Correlation (CRITIC) method in conjunction with two ranking methodologies: Combinative Distance-Based Assessment (CODAS) and Measurement of Alternatives and Ranking according to Compromise Solution (MARCOS), to objectively determine attribute weights. This approach enabled comprehensive prioritization of the alternatives. The study examined various compositions by altering the weight percentages of BFF and MF, along with different levels of benzoyl chloride surface treatment. Using basic mechanical performance criteria—including ultimate tensile strength (TS), ultimate flexural strength (FS), and impact strength (IS)—the load-bearing capacity and energy absorption properties of natural fiber-reinforced polymer composites were assessed. Based on these criteria, the alternatives were evaluated.

CRITIC analysis

The CRITIC method is an impartial weighting tool. The methodology employed for determining attribute weights using the CRITIC technique is outlined as follows [24]:

The CRITIC weighting approach begins with the normalization of the decision matrix using the following formulas:

Step 1 Decision matrix. The establishment of a decision matrix involves specifying a set of *q* criteria and *p* alternatives, which are then integrated into multi-criteria methods as described.

$$[Z_{ij}]_{p\times q} = \begin{matrix} \\ A_1 \\ A_2 \\ \vdots \\ A_i \\ \vdots \\ A_p \end{matrix} \begin{bmatrix} c_1 & C_2 & \cdots & C_j & \cdots & C_q \\ Z_{11} & Z_{12} & \cdots & Z_{1j} & \cdots & Z_{1q} \\ Z_{21} & Z_{22} & \cdots & Z_{2j} & \cdots & Z_{2q} \\ \vdots & \vdots & \cdots & \vdots & \cdots & \vdots \\ Z_{i1} & Z_{i2} & \cdots & Z_{ij} & \cdots & Z_{iq} \\ \vdots & \vdots & \cdots & \vdots & \cdots & \vdots \\ Z_{p1} & Z_{p2} & \cdots & Z_{pj} & \cdots & Z_{pq} \end{bmatrix} \quad (2)$$

Where, Z_{ij} represents the range of the i[th] choice for the j[th] criteria.

Step 2 Normalization of decisional matrix. The organized decisional matrix is normalized for the advantageous (N_b) and disadvantageous (N_{nb}) criteria:

$$r_{ij} = \frac{z_{ij} - \min(z_{ij})}{\max(z_{ij}) - \min(z_{ij})} \nearrow^{\text{if}}\ j \in N_b \quad (3)$$

$$r_{ij} = \frac{\max(z_{ij}) - z_{ij}}{\max(z_{ij}) - \min(z_{ij})} \nearrow_{if}\ j \in N_{nb} \quad (4)$$

Step 3 The dispersion degree is measured by the standard deviation (S_j) of each criterion, as evaluated by the subsequent formula:

$$\begin{cases} S_j = \sqrt{\frac{\sum_{i=1}^{p} (r_{ij} - \bar{r}_j)^2}{p-1}} \\ \overline{r_j} = \frac{\sum_{i=1}^{p} r_{ij}}{p} \end{cases} \quad (5)$$

Step 4 The subsequent formula is used to evaluate the degree of conflict between the criteria.

$$\Re_j = \sum_{i=1}^{q} (1 - \nu_{ij}) \quad (6)$$

Where ν_{ij} represent the correlation coefficient between i[th] and j[th] criteria.

Step 5 Weight calculation

The formula for j[th] criterion weight calculation is given as:

$$\omega_j = \frac{\Re_j \times S_j}{\sum_{j=1}^{q} \Re_j \times S_j} \quad (7)$$

CODAS analysis

The computing process for the CODAS approach encompassed the following steps [25]:

Step 1 Standardize the criterion: A decision matrix is formulated by eq. (1). To eliminate the bias arising from different measurement units, it is essential to standardize the criterion values to a consistent scale. This is achieved by applying suitable normalization techniques, as shown below:

Equation (8) is then used to normalize the performance matrix, $P_{ij}^{m\times n}$, to $PN_{ij}^{m\times n}$.

$$\mathrm{PN}_{ij} = \begin{cases} \frac{\mathrm{P}_{ij}}{\max \mathrm{P}_{ij}} \text{ if } j \in \text{beneficial attribute} \\ \frac{\min \mathrm{P}_{ij}}{\mathrm{P}_{ij}} \text{ if } j \in \text{non} - \text{ beneficial attribute} \end{cases} \quad (8)$$

Step 2-Evaluate the weightage normalized distance: The weighted normalized performance matrix $w_{ij}^{m\times n}$ is obtained by multiplying each normalized value PN_{ij} with its corresponding criterion weight w_j. This step integrates both the performance and significance of each criterion in the evaluation process.

$$\omega_{ij} = \omega_j \times \mathrm{PN}_{ij} \quad (9)$$

Whereas ω_j. is the weighted average of the j[th] criteria, as determined by Equation.

Step 3-Calculate the negative-ideal solution: The negative-ideal solution for each criterion is determined by selecting the minimum value, representing the least favorable performance. This distinction aids in evaluating the minimum achievable performance level: To determine the negative ideal point (NIP_j), the following formula is used.

$$\mathrm{NIP}_j = \min_i \omega_{ij} \quad (10)$$

Equations (11) and (12) are employed to calculate the Euclidean distance and the Taxicab distance for the selections from NIP_j:

$$\mathrm{E}_i == \sqrt{\sum_{j=1}^{n} \left(\omega_{ij} - \mathrm{NIP}_j\right)^2} \quad (11)$$

$$\mathrm{T}_i = \sum_{j=1}^{n} \left|\omega_{ij} - \mathrm{NIP}_j\right| \quad (12)$$

Step 5-Calculate the valuation matrix: The subsequent step is to generate the evaluation matrix $E_{ik}^{m\times m}$ using Eq. (13) after evaluating the E_i and T_i for each alternative:

$$[\Re_{ik}]_{m\times m} = (\mathrm{E}_i - \mathrm{E}_k) + \zeta(\mathrm{E}_i - \mathrm{E}_k) \times (\mathrm{T}_i - \mathrm{T}_k) \quad (13)$$

whereas ζ ($0.01 \le \zeta \le 0.05$) k and $\in$ {1, 2, ..., m} is the threshold parameter.

($\zeta = 0.02$)

Step 6-Evaluate the total assessment score: An overall score or utility value is determined by aggregating the weighted distances of each alternative, frequently through a summation approach. The options are arranged in descending order based on their scores, with higher scores indicating superior performance. Eq. (14) is used to calculate the assessment score Ω_i, and the options are arranged in descending order of Ω_i.

$$\Omega_i = \sum_{k=1}^{m} \Re_{ik} \quad (14)$$

Measurement of Alternatives and Ranking according to Compromise Solution (MARCOS)

The MARCOS model is employed to address many decision-making challenges due to its straightforward computations. The following steps outline the MARCOS technique [26].

Step 1: Decision matrix. A decisional matrix is formulated by eq. (1). The basic choice matrix ($Z_{ij}^{p\times q}$.) is augmented by incorporating the Ideal Value (IV) and Anti-Ideal Value (AIV), resulting in an augmented

matrix.

The IV and AIV are ascertained using the subsequent formulae.

$$IV = \text{maximum}\left(Z_{ij}\right) \nearrow \text{ if } j \in N_b, \text{ and } IV = \text{minimum}\left(Z_{ij}\right) \nearrow \text{ if } j \in N_{nb} \quad (15)$$

$$AIV = \text{maximum}\left(Z_{ij}\right) \nearrow \text{ if } j \in N_{nb}, \text{ and } AIV = \text{minimum}\left(Z_{ij}\right) \nearrow \text{ if } j \in N_b \quad (16)$$

Step 2 The following formula is used to normalize the revised decision matrix within the range of 0-1.

$$z_{ij} = \frac{z_{ij}}{z_{IV}} \nearrow \text{ if } j \in N_b \quad (17)$$

$$z_{ij} = \frac{z_{IV}}{z_{ij}} \nearrow \text{ if } j \in N_{nb} \quad (18)$$

Step 3 The subsequent equation is employed to create the weighted normalized decision matrix.

$$\varpi_{ij} = \omega_j \times z_{ij} \quad (19)$$

Step 4 Computation of the summation of the weighted matrix utilizing the subsequent equation.

$$k_i = \sum_{i=1}^{p} \varpi_{ij} \quad (20)$$

Step 5 Assessment of the utility value of alternatives. The following formula is used to calculate the utility degrees for IV and AIV.

$$k_i^+ = \frac{k_i}{k_{IV}}, \text{ and } k_i^- = \frac{k_i}{k_{AIV}} \quad (21)$$

Step 6 The utility functions for the IV and AIV are established using the following formula.

$$f(k_i^+) = \frac{k_i^-}{k_i^+ + k_i^-}, \text{ and } f(k_i^-) = \frac{k_i^+}{k_i^+ + k_i^-} \quad (22)$$

Step 7 The subsequent formula is employed to obtain the ultimate utility function of alternatives.

$$f(k_i) = \frac{k_i^+ + k_i^-}{1 + \frac{1-f(k_i^+)}{f(k_i^+)} + \frac{1-f(k_i^-)}{f(k_i^-)}} \quad (23)$$

Step 8 Alternatives are ranked in descending order based on their f_{ki}. values, from best to worst.

Results and Discussions

Results on FTIR analysis

Figure 5(a) displays the FTIR spectra of raw and benzoyl chloride-treated natural fibers at concentrations of 3 wt% and 6 wt%, highlighting the chemical changes due to surface functionalization. The untreated fiber spectrum shows a broad and intense absorption band centered at 3342 cm^{-1}, attributed to O–H stretching vibrations from hydroxyl groups in hemicellulose, cellulose, and lignin. The peak at 2894 cm^{-1} corresponds to C–H stretching vibrations of aliphatic –CH and $–CH_2$ groups, while the distinct band at 1735 cm^{-1} is assigned to C=O stretching of acetyl and uronic ester groups in hemicellulose. The band at 1244 cm^{-1} indicates C–O stretching of aryl-ether linkages, a characteristic feature of the lignin structure. These spectral features confirm the complex lignocellulosic nature of the untreated fiber. After treatment with 3 wt% benzoyl chloride, a shift in the O–H stretching band to 3351 cm^{-1}, along with a reduction in intensity, indicates partial esterification of hydroxyl groups. The disappearance of the 1735 cm^{-1} signal suggests the removal or chemical modification of hemicellulose, likely due to hydrolysis or transesterification under alkaline conditions. A new peak at 1305 cm^{-1} indicates aromatic C–C or C–O stretching, confirming the incorporation of benzoyl groups into the fiber matrix. In the 6 wt% benzoylated sample, more pronounced changes occur. The O–H band shifts to 3354 cm^{-1} and becomes significantly weaker, implying a higher degree of substitution. New aromatic bands at 1362 cm^{-1} and 1308 cm^{-1} are attributed to the skeletal vibrations of aromatic ring structures, confirming an increased presence of benzoyl functionalities. The complete disappearance of the carbonyl peak at 1735 cm^{-1} further supports the removal of hemicellulose, indicating that higher benzoylation levels promote better matrix purification and functionalization. FTIR analysis demonstrates that benzoylation reduces polar functional groups and introduces aromatic moieties, enhancing the hydrophobicity and their compatibility of the fibers with polymer matrices.

Figure 5(b) shows the FTIR spectra of raw and benzoylated BFF illustrating changes in chemical structure and functional groups due to benzoylation at 3 wt% and 6 wt%. A strong absorption band at 3338 cm^{-1} in the raw fiber is due to O–H stretching vibrations of intermolecular hydrogen bonds in hemicellulose and cellulose. The 2892 cm^{-1} peak arises from C–H stretching in aliphatic chains. The band at 1605 cm^{-1} corresponds to aromatic C=C stretching in lignin, while the peaks at 1324 cm^{-1} and 1257 cm^{-1} are due to C–O and aryl-ether vibrations, respectively. A peak at 902 cm^{-1} confirms the presence of β-glycosidic linkages in cellulose. Upon benzoylation with 3 wt% and 6 wt% benzoyl chloride, a noticeable reduction in the O–H peak intensity (shifted to 3316 cm^{-1}) indicates substitution of hydroxyl groups by esterification. Enhanced peaks at 1324 cm^{-1}, 1257 cm^{-1}, and 1162 cm^{-1} suggest aromatic ring vibrations, confirming successful benzoyl group incorporation. A new peak at 1028 cm^{-1} reflects changes in C–O and C–O–C stretching regions. These modifications confirm successful surface functionalization, particularly at 6 wt%, which improves hydrophobicity and enhance the fiber–matrix bonding in composite applications.

The FTIR Spectra of raw and benzoyl treated fibre (Fig. 5c) reveals significant chemical modifications induced by surface treatment. The untreated fibre

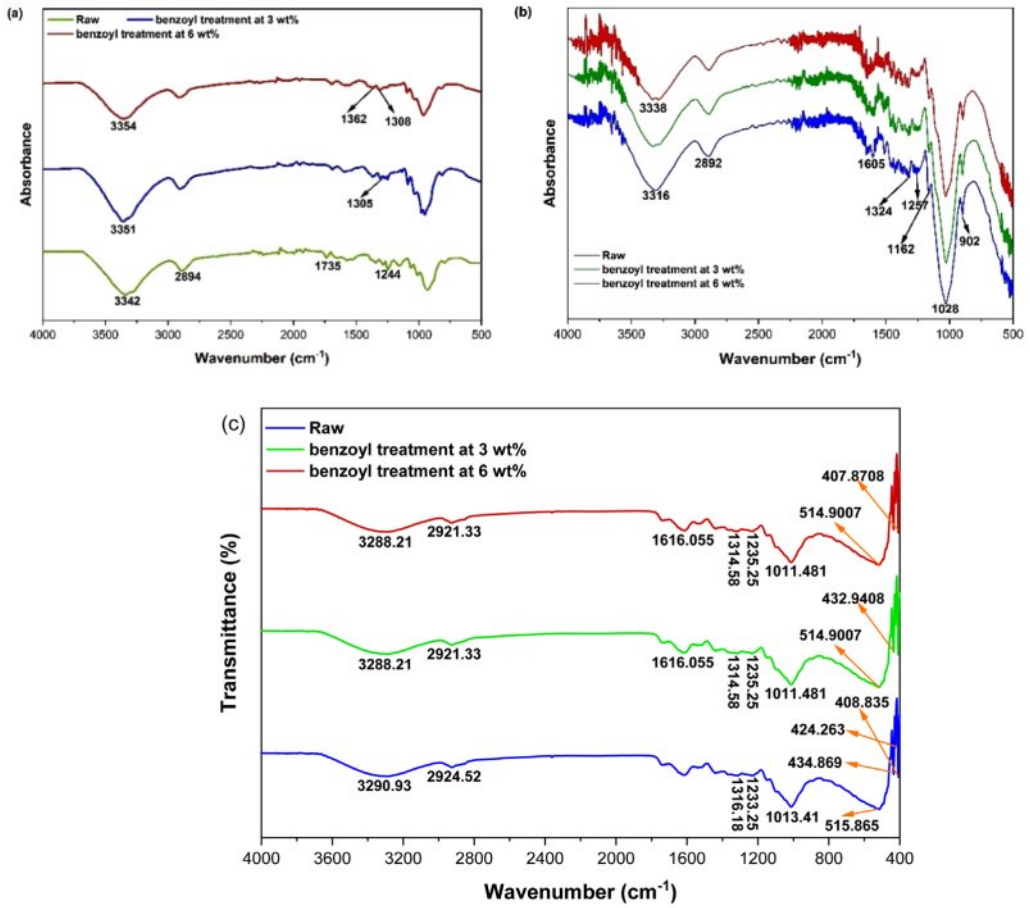

Fig. 5. FTIR analysis of (a) Madar fibre, (b) Borassus fruit fibre and (c) lotus seed powder of raw and benzoyl treatment at 3 wt% and 6 wt%.

exhibits a broadband at 3290.93 cm^{-1} corresponding to the stretching vibrations of -OH groups present in cellulose, hemicellulose and lignin. This band slightly shifts to 3288.21 cm^{-1} for 3 wt.% and 6 wt.% benzoyl treated fibers, indicating partial substitution or reduction of hydroxyl functionalities due to esterification between benzoyl chloride and the fibre's hydroxyl groups. The peaks at 2924.52–2921.33 cm^{-1} correspond to C-H asymmetric stretching of methyl and methylene groups, confirming the presence of aliphatic structures. The peak near 1616.05 cm^{-1} is attributed to aromatic C=C stretching and conjugated carbonyl (C=O) vibrations, which become more pronounced after benzoylation, reflecting enhanced aromaticity from the benzoyl group attachment. The absorption bands at 1233.25–1235.38 cm^{-1} and 1316.18–1314.58 correspond to C-O-C and C-O stretching in cellulose and lignin backbones, both of which slightly decrease in intensity following treatment, suggesting partial removal of hemicellulose and amorphous components. Additional peaks observed at 1013.41–1011.481 cm^{-1} are associated with polysaccharide C-O vibrations, while the bands at 514.9007–407.8708 cm^{-1} correspond to aromatic ring deformation and C-H bending. The shift and intensity reduction in these characteristic peaks collectively confirm that benzoyl treatment effectively reduces the hydrophilic -OH groups and enhances the fibers surface hydrophobicity, thereby improving interfacial adhesion potential in polymer composite matrices.

Optimization

The objective of this investigation is to optimize the hybrid fibers and surface treatments for varying weight ratios. The Taguchi method was employed to assess the optimization of BFF and MF. The establishment of five parameters led to the development of 16 composite plates.

Table 1 presents the parameters at different levels, whereas Table 2 displays the constructed L9 orthogonal array (OA) and signal-to-noise (S/N) ratio used in the

Table 1. Experimental input factors and its levels.

Factors	Factor Code	Levels		
		1	2	3
Madar fibre (wt%)	A	0	6	12
Borassus fruit fibre (wt%)	B	0	6	12
Benzoyl chloride treatment (wt%)	C	0	3	6
LSSP (wt%)	D	2	3	4

Table 2. Taguchi optimization of Borassus fruit/Madar composites utilizing the L9 orthogonal array.

Sl. No.	A: (wt.%)	B: (wt.%)	C: (wt.%)	D: (wt %)	TS (MPa)		FS (MPa)		IS (J/m)	
					Actual	SN ratio	Actual	SN ratio	Actual	SN ratio
1	0	0	0	2	29.45	29.38	47.54	33.54	55.37	34.87
2	0	6	3	3	33.84	30.59	52.06	34.33	65.54	36.33
3	0	12	6	4	35.64	31.04	53.27	34.53	67.24	36.55
4	6	0	3	4	34.2	30.68	50.45	34.06	65.09	36.27
5	6	6	6	2	36.11	31.15	56.74	35.08	70.82	37.00
6	6	12	0	3	36.12	31.16	52.26	34.36	68.45	36.71
7	12	0	6	3	35.05	30.89	57.43	35.18	71.26	37.06
8	12	6	0	4	36.61	31.27	59.74	35.53	68.66	36.73
9	12	12	3	2	38.6	31.73	63.25	36.02	69.63	36.86

analysis of mechanical properties. The L9 OA was employed to ascertain the properties, with the highest signal-to-noise ratio yielding the best outcomes. The maximum tensile strength (TS) of 38.6 MPa was attained in the ninth trial by treating Borassus fruit and Madar fibers with 3 wt% benzoyl chloride and 2 wt% LSSP, each at a concentration of 12 wt%. In the ninth and seventh trials, the maximum flexural strength (FS) and impact strength (IS) values were 63.25 MPa and 71.26 J/m, respectively. In a prior analysis, the use of MF (28 wt%) and sugarcane bagasse ash (7 wt%) as fillers in epoxy via compression molding showed enhanced mechanical performance of TS (61 MPa), FS (147 MPa), and IS (54 kJ/m²) [27].

Results on tensile strength of hybrid composite

The tensile strength (TS) of the fabricated composites indicated that TS increased with the addition of BFF and MF. The reinforcing 12 wt% BFF, 12 wt% MF, 6 wt% BT, and 4 wt% LSSP demonstrated the optimal TS values. The use of fibers improved the TS of the fabricated composites. The integration of BFF and MF within an optimal range enhanced the tensile characteristics of the hybrid composites. The signal-to-noise (S/N) ratios of BFF and MF increased from 31 to 31.3 and from 31 to 31.31, respectively by adding upto 12 wt% of each fiber as shown in Fig. 6.

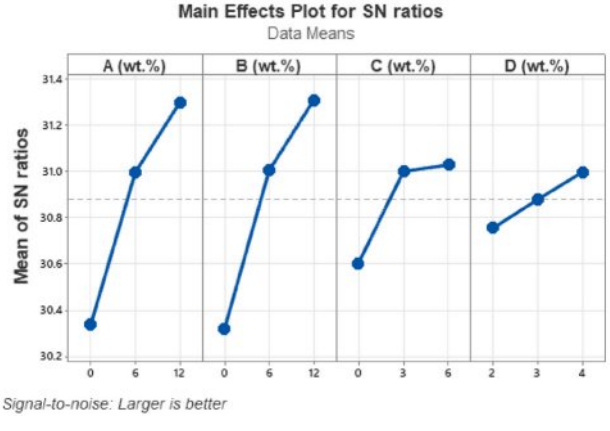

Fig. 6. Main effect plot for tensile strength (TS) (S/N ratio).

The tensile characteristics of the polymer-based composites were substantially enhanced by the addition of hybrid fiber reinforcement at a concentration of up to 24 wt%. The treated fibers with benzoyl chloride also contributed to the increase in ultimate tensile strength. After treatment with benzoyl chloride, the S/N ratio of the final tensile strength increased from 29.38 to 31.73, suggesting that the surface exhibited favorable characteristics. Benzoyl treatment reduced the hydrophilic nature of the natural fiber composites by substituting benzoyl groups for hydroxyl groups. The tensile strength improved only up to 12 wt% BFF/MF because this represents the optimum fiber loading for effective stress transfer and uniform dispersion within the epoxy matrix. Beyond this level, fibers tend to agglomerate and overlap, leading to poor wetting, void formation, and stress concentration zones that hinder load distribution. Additionally, excessive fiber content reduces matrix continuity, weakening the interfacial bonding and resulting in a decline in tensile strength. Thus, 12 wt% provided the best balance between fiber reinforcement and matrix integrity, ensuring maximum tensile efficiency.

As a result, the fibers developed a grainy texture due to surface treatment, which improved the adhesive characteristics at the fiber–epoxy interface and facilitated resin infiltration. Consequently, the polymer-based composites exhibited robust interfacial bonding.

Results on flexural strength of hybrid composite

The improvement in flexural strength (FS) is due to the increased weight percentage of Borassus fruit fibers. Fig. 7 shows that adding 12 wt% BFF raised the signal-to-noise (S/N) ratio from 34.50 to 35.58. This improvement can be attributed to the homogeneous dispersion of fibers in the epoxy-based composites. Adding MF to the composites at concentrations of up to 12 wt% enhanced their flexural properties and increased the S/N ratio from 34.98 to 34.97. The hydrophilic characteristics of the

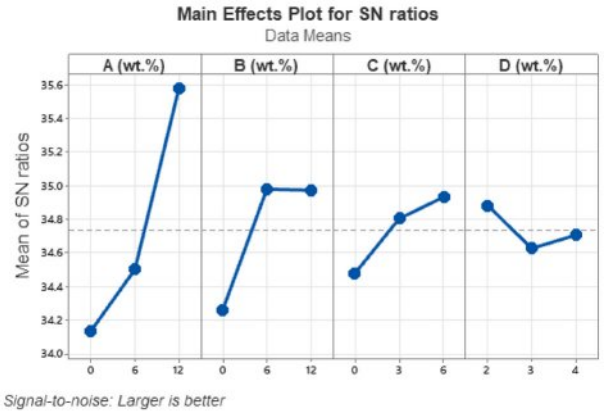

Fig. 7. Main effect plot for flexural strength (FS) (S/N ratio).

fiber reinforcement were reduced as a result of benzoyl chloride treatment, thereby improving the fiber–matrix interaction. Flexural strength showed smaller S/N ratio changes because it is less sensitive to fiber alignment and interfacial defects. During bending, the matrix supports more load, reducing variability, whereas tensile strength depends directly on fiber–matrix bonding, making it more sensitive to parameter changes.

Combining 12 wt% BFF and 12 wt% MF with 6 wt% BT and 2 wt% LSSP resulted in optimal flexural properties. The flexural performance was positively influenced by the weight percentage of BFF and MF. The application of benzoyl chloride significantly improved the interaction between the fiber and matrix, leading to reduced porosity and fewer surface irregularities in the polymer-based composites. The S/N ratio increased from 34.87 to 36.86 as a consequence of the surface treatment.

Results on Impact strength of hybrid composite

The impact characteristics of the composites were evaluated using impact strength (IS), as shown in figure 8. An increase in the impact strength of the epoxy-based composites was observed due to the incorporation of reinforcing fibers. The treatment with benzoyl chloride

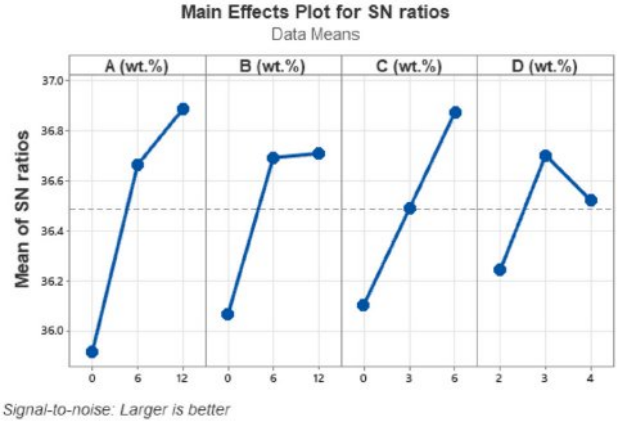

Fig. 8. Main effect plot for impact strength (IS) (S/N ratio).

Table 3. Results on CRITIC analysis.

	TS	FS	IS
STD	0.276	0.314	0.303
Cj	0.076	0.130	0.112
Wj	0.239	0.408	0.352

significantly improved the impact strength of the fibers. Effective adhesion between the fibers and the matrix was achieved through the addition of MF and BFF, resulting in enhanced impact characteristics.

The maximum IS value was observed for the composite with 12 wt% BFF, 12 wt% MF, 6 wt% BT, and 3 wt% LSSP. Similarly, recent studies reported optimum properties in hybrid vinyl ester composites treated with $KMnO_4$, comprising 30 wt% Borassus fruit fiber, 30 wt% cigarette butt fiber, and 5 wt% eggshell powder [28] The results indicate that the addition of Madar fibers beyond a certain threshold reduced the IS value. Fibers were effectively incorporated into the interstitial space of polymer-based composites up to an overall substitution of 24 wt%.

CRITIC Results

The normalization of the data was executed by using eq. (3). The standard deviations (σ_j) for each criterion are presented in Table 3 and it was computed using eq. (4). Eq. (6) was employed to determine the data measure values, as illustrated in Table 3. Subsequently, the criterion weights were calculated using eq. (7) and are presented in Table 3.

Multi-response optimization using CODAS

The current study includes three alternatives and nine criteria, therefore n=3 and m=9. Table 4 presents the performance matrix [P_{ij}.] subsequent to its normalization by eq. (7). Table 4 illustrates the weighted normalized performance matrix [P_{ij}.] computed in the subsequent phase using eq. (9). As a result, an anti-ideal solution was generated and documented in Table 4 for each scenario. Eqs. (11) and (12) were then employed to calculate E_i and the T_i respectively as shown in Table 4. The relative-assessment matrix was generated by applying Eq. (13).

Following the computation of the E_i and the T_i, Eq. (14) was used to determine the assessment score Ω_i for all alternatives. The results are displayed in Table 4. The Ω_i values in Table 4 indicate that the alternatives were ultimately arranged in descending order of benefit. The enhanced mechanical properties obtained through the CODAS method were observed in the combination containing 12 wt% BFF, 12 wt% MF, 3 wt% BT, and 2 wt% LSSP (ninth trial combination). Since CODAS calculations involve negative values and complex distance-based operations, the analysis was conducted in Excel, which is better suited than Minitab for handling such computations.

Table 4. CODAS of BFF/MF hybrid combinations.

S.No	Normalization			Weighted Normalization			Ei	Ti	Assessment Score	Rank
	TS	FS	IS	TS	FS	IS				
1	0.763	0.752	0.777	0.182	0.307	0.274	0.0000	0.000	-0.742	9
2	0.877	0.823	0.920	0.210	0.336	0.324	0.0641	0.107	-0.167	7
3	0.923	0.842	0.944	0.221	0.344	0.332	0.0792	0.134	-0.031	6
4	0.886	0.798	0.913	0.212	0.325	0.322	0.0594	0.096	-0.210	8
5	0.935	0.897	0.994	0.224	0.366	0.350	0.1051	0.177	0.202	4
6	0.936	0.826	0.961	0.224	0.337	0.338	0.0825	0.136	-0.002	5
7	0.908	0.908	1.000	0.217	0.370	0.352	0.1069	0.177	0.218	3
8	0.948	0.945	0.964	0.227	0.385	0.339	0.1117	0.189	0.261	2
9	1.000	1.000	0.977	0.239	0.408	0.344	0.1358	0.228	0.479	1
			Negative	0.182	0.307	0.274				

Multi-response optimization using MARCOS method

The choice matrix was constructed by determining the ideal value (IV) and anti-ideal value (AIV) using eq. (15) and (16). Table 5 illustrates the structured decision matrix of the MARCOS analysis for the designated alternatives and criteria. Eqs. (17) and (18) are implemented to normalize each value in accordance with the MARCOS process. Table 5 shows the normalized decision matrix for the MARCOS analysis. As shown in Table 3, the weights are derived from the CRITIC method and are subsequently used to construct the weighted decision matrix by using eq. (19). Consequently, the utility degree (k_{i+}, k_{i-}) and the utility functions $f(k_{i+})$, $f(k_{i-})$ for the alternatives are determined by employing Eqs. (20)-(22) of the MARCOS approach. Consequently, Eq. (23) is then used to determine the ultimate utility function, $f(k_i)$ for each option. The findings of the MARCOS investigation are summarized in Table 5. This research employed the CRITIC and MARCOS methods to rank brake friction composites reinforced with rice husk, ash, and Grewia optiva fiber based on tests aligned with SAE standards. Validation confirmed the reliability of the integrated MCDM approach for material selection [29].

The ninth run combination of 12 wt% BFF, 12 wt% MF, 3 wt% BT, and 2 wt% LSSP exhibited the highest mechanical properties, as evidenced by the comparable findings of the multi-response optimization with MARCOS (Table 5). The ninth composite is identified as the overall optimal formulation because the optimization framework (CRITIC–CODAS–MARCOS) evaluates all mechanical properties collectively rather than individually. Although it ranks seventh in impact strength (IS), it achieves consistently high performance across tensile and flexural strengths and maintains

Table 5. MARCOS method of BFF/MF hybrid combinations.

S.No	Normalization			Weighted Normalizaton			Ki	utility degrees		utility functions	f (ki-)	f(ki+)/ f(ki+)	f(ki-)/ f(ki-)	f(ki)	Rank
	TS	FS	IS	TS	FS	IS		Ki+	Ki-	f (ki+)					
1	0.763	0.752	0.777	0.182	0.307	0.274	0.763	0.769	1.000	0.565	0.435	0.769	1.300	0.577	9
2	0.877	0.823	0.920	0.210	0.336	0.324	0.869	0.877	1.140	0.565	0.435	0.769	1.300	0.657	7
3	0.923	0.842	0.944	0.221	0.344	0.332	0.896	0.905	1.176	0.565	0.435	0.769	1.300	0.678	6
4	0.886	0.798	0.913	0.212	0.325	0.322	0.859	0.867	1.126	0.565	0.435	0.769	1.300	0.649	8
5	0.935	0.897	0.994	0.224	0.366	0.350	0.939	0.948	1.232	0.565	0.435	0.769	1.300	0.710	4
6	0.936	0.826	0.961	0.224	0.337	0.338	0.899	0.907	1.179	0.565	0.435	0.769	1.300	0.680	5
7	0.908	0.908	1.000	0.217	0.370	0.352	0.939	0.948	1.232	0.565	0.435	0.769	1.300	0.710	3
8	0.948	0.945	0.964	0.227	0.385	0.339	0.951	0.960	1.247	0.565	0.435	0.769	1.300	0.719	2
9	1.000	1.000	0.977	0.239	0.408	0.344	0.991	1.000	1.300	0.565	0.435	0.769	1.300	0.749	1
						IV	0.991								
						AIV	0.763								

Table 6. MARCOS response table.

Level	A (wt.%)	B (wt.%)	C (wt.%)	D (wt.%)
1	0.6372	0.6454	0.6585	0.6787
2	0.6798	0.6956	0.6852	0.6824
3	0.7263	0.7023	0.6995	0.6821
Delta	0.0891	0.0568	0.0410	0.0037
Rank	1	2	3	4

balanced overall property values. In multi-criteria optimization, such composites with uniformly strong, well-distributed properties are prioritized over those excelling in a single parameter but performing poorly in others. Hence, the ninth composite is considered optimal due to its superior overall performance index, not merely its IS ranking.

The MARCOS response table (Table 6) demonstrates that, the mechanical properties of epoxy-based composites are significantly enhanced by reinforced natural fibers. The weight percentage of BFF and MF significantly improves the overall mechanical characteristics of polymer-based composites. In the MARCOS optimization, the 6 wt% BT was ranked third. The enhanced mechanical properties achieved with MARCOS were observed in the formulation comprising 12 wt% BFF, 12 wt% MF, 6 wt% BT, and 3 wt% LSSP (Table 6).

Fig. 9 illustrates the interaction plot of the evaluation score (derived from CODAS) and f(ki) (derived from MARCOS) revealing a similar trend present in the MARCOS data. A comparable MARCOS approach was employed in other studies on natural fiber-reinforced composites for optimization.

The MARCOS procedure achieved the optimal mechanical performance with the combination of 12 wt% BFF, 12 wt% MF, 6 wt% BT, and 3 wt% LSSP. The combination demonstrated an IS of 69.63 J/m, FS of 63.25 MPa, and TS of 38.6 MPa. These results were superior to those of other combinations. In MARCOS analysis, alternatives are ranked based on their overall utility score, which considers all weighted performance

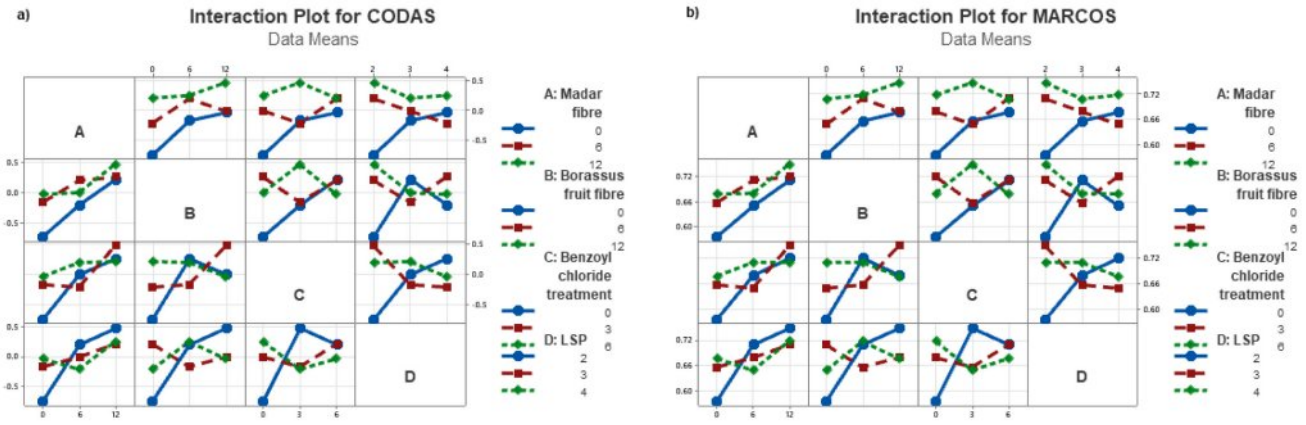

Fig. 9. Interaction plot for CODAS results (Ωi) and MARCOS results (f(ki)) (assessment score) using Minitab 20.2.

Table 7. Sensitivity analysis.

	A1	A2	A3	A4	A5	A6	A7	A8	A9
CODAS									
Actual condition	-0.742	-0.167	-0.031	-0.210	0.202	-0.002	0.218	0.261	0.479
Ranking	A9<A8<A7<A5<A6<A3<A2<A4<A1								
C1	0.712	0.915	1.062	0.961	1.083	1.102	0.983	1.155	1.363
Ranking	A9<A8<A7<A5<A6<A3<A2<A4<A1								
C2	0.693	1.023	1.146	1.062	1.223	1.224	1.170	1.144	1.254
Ranking	A9<A6<A5<A7<A3<A8<A4<A2<A1								
MARCOS									
Actual condition	0.577	0.657	0.678	0.649	0.710	0.680	0.710	0.719	0.749
Ranking	A9<A8<A7<A5<A6>A3<A2<A4<A1								
C1	0.576	0.656	0.677	0.648	0.708	0.679	0.707	0.719	0.750
Ranking	A9<A8<A5<A7<A6<A3<A2<A4<A1								
C2	0.578	0.665	0.689	0.661	0.717	0.694	0.714	0.720	0.748
Ranking	A9<A8<A5<A7<A6<A3<A2<A4<A1								

criteria, not just tensile strength (TS). Hence, a sample with slightly lower TS may rank higher if it performs better in other parameters—like flexural or impact strength—that have higher relative weights assigned by the CRITIC method. This reflects MARCOS's focus on balanced multi-criteria performance rather than dominance in a single property.

Sensitivity analysis

To assess the influence of weights on the final ranking of the alternatives, the weights are interchanged. A sensitivity study was performed by adjusting the weights of the composite mechanical properties to evaluate their impact on the final ranking. This study examines the effect of weight variation under two specified condition, as presented in Table 7. The current weights of TS, FS and IS are 0.239, 0.408, and 0.344, respectively. In condition 1 (C1), the weights assigned to TS, FS and IS are 0.408, 0.352, and 0.239, respectively. In condition 2 (C2), the weights assigned to TS, FS and IS are 0.352, 0.239, and 0.408, respectively. Table 7 demonstrates that modifying the weights exerts a negligible influence on the rankings, as the top three alternatives consistently remain the same across all three scenarios.

Microstructural analysis

The specimens were analyzed using SEM, as illustrated in Fig 10. Fig. 10(b) illustrates the effects of a 0 wt% MF, 6 wt% BFF, and a 3 wt% BT. Fiber debonding, matrix fracture, fiber pullouts, and void gaps were identified in the presence of 6 wt% MF, 0 wt% BFF, and 3 wt% BT. Natural fiber amalgamations demonstrated these surface deformations. The mechanical properties of the composites were reduced due to the non-homogeneous distribution of single fiber reinforcement from natural fibers within the matrix, which cause the surface deformations. The hybridization of BFF and MF resulted in a more uniform distribution of fibers throughout the matrix, thereby enhancing the overall qualities. In particular, the combination of 12 wt% MF, 12 wt% BFF, and 3 wt% BT (Fig. 10c) exhibited the enhanced tensile strength. The favorable attributes of the optimal formulation, which was derived from the CODAS and MARCOS methods and included 12 wt% MF, 12 wt% BFF, and 6 wt% BT (Fig. 8d), were primarily due to the reduced hydrophilicity resulting from the 6 wt% BT. The slight hydrophobic nature of the resin reduces bonding with hydrophilic of the natural fibers. Appropriate surface treatment produces a grainy texture on the fibers, which optimizes the mechanical properties of the polymer composites and improving bonding with the epoxy matrix. SEM images confirmed uniform filler dispersion and fibrillated fiber structure, validating its performance suitability [30]. Voids formed

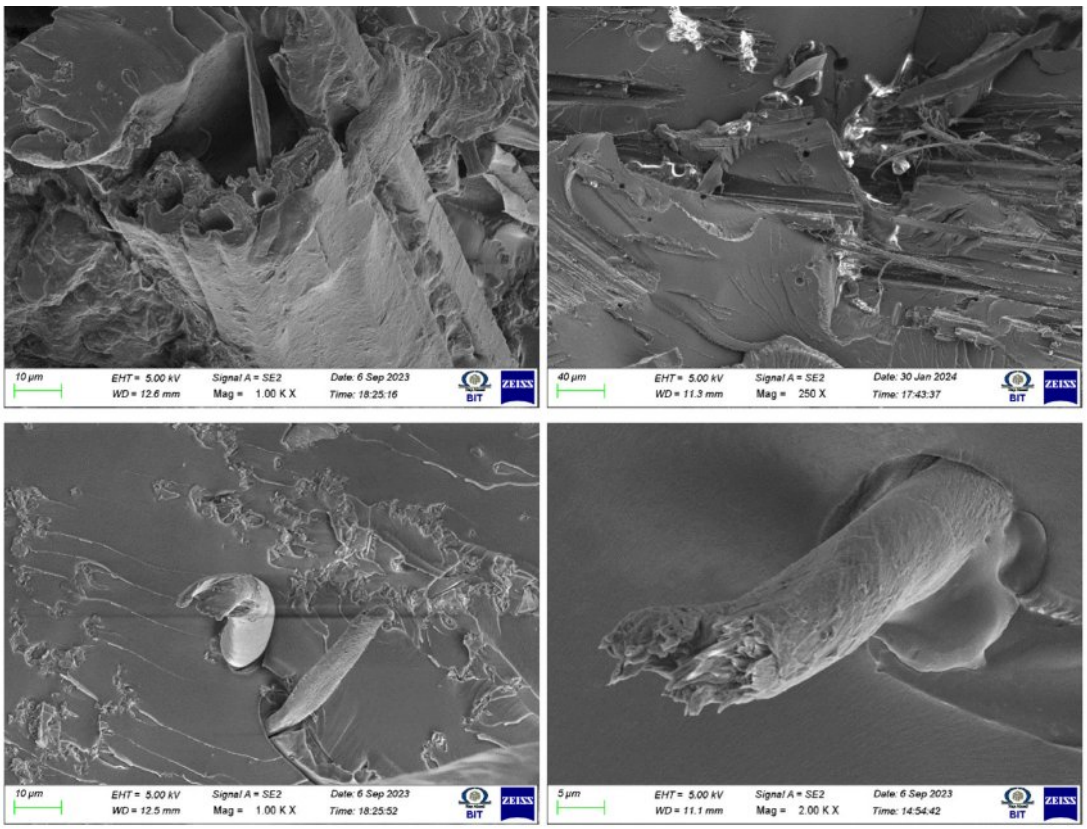

Fig. 10. SEM analysis of (a) 0 wt% MF+6 wt% BFF+3 wt% LSSP +3 wt% BT, (b) 6 wt% MF+0 wt% BFF+3 wt% LSSP +3 wt% BT, (c) 12 wt% MF+12 wt% BFF+3 wt% LSSP +3 wt% BT, (d) 12 wt% MF+12 wt% BFF+3 wt% LSSP +6 wt% BT after tensile-tested composites.

during fabrication typically appear as smooth, round, or irregular air pockets within the matrix, resulting from trapped air or incomplete resin wetting during layup. In contrast, fiber pullout observed after testing shows elongated cavities or imprints with clear fiber traces or resin debris along the walls, indicating that fibers were dislodged under mechanical loading.

Conclusions

This study evaluated the mechanical properties of epoxy polymer composites containing BFF and MF both untreated or treated with benzoyl chloride. For the purpose of manufacturing, the hand layup technique was implemented, and the optimal conditions for overall mechanical characteristics of the composite were determined using Taguchi-based CODAS and MARCOS methodologies. The following four variables were BFF (0 to 12 wt%), MF (0 to 12 wt%), LSSP (2 to 4 wt%) and BT (0 to 6 wt%). The following results were obtained by employing a L9 orthogonal array to evaluate the optimal outcomes.

The treatment with benzoyl chloride significantly reduced the intensity and slightly modified the O–H stretching bands, thereby confirming the effective esterification. In MF, the O–H peak shifted from 3342 cm^{-1} to 3354 cm^{-1}, while in BFF, it shifted from 3338 cm^{-1} to 3316 cm^{-1}. The absents of the 1735 cm^{-1} carbonyl band in MF, along with the presence of aromatic peaks (1305–1362 cm^{-1}) in both fibers, validates the successful integration of benzoyl groups. The spectral changes demonstrate enhanced hydrophobicity and improved interfacial compatibility with polymer matrices, confirming the efficacy of benzoylation for composite applications.

The response table of CODAS and MARCOS indicates that the overall mechanical properties of the hybrid composites were significantly enhanced by BFF.

An enhanced mechanical property was reported utilizing the MARCOS method in a treatment including 12 wt% BFF, 12 wt% MF, 6 wt% BT, and a 3 wt% LSSP combination.

The mechanical strength of epoxy-based composites was enhanced by the integration of BFF and MF, which also enhanced compatibility with the reinforcement/ matrix phase.

The hydrophilicity of lignocellulosic fibers was reduced and their adherence to polymer matrix composites was improved through the use of benzoyl chloride for surface treatment.

According to scanning electron microscopy (SEM) analysis, integrating natural fiber reinforcement into a matrix causes deformations and an uneven distribution and this reduces the mechanical properties of the composites. The hybridization of BFF and MF improved the properties of the matrix due to homogeneous distribution of the fibers.

The optimized formulation comprising 12 wt% MF, 12 wt% BFF, 3 wt% LSSP and 6 wt% BT derived from the CODAS and MARCOS methods, exhibited favorable features attributable to hybridization and a decrease in hydrophilicity resulting from 6 wt%. benzoyl chloride surface treatment.

The most optimal combinations are appropriate for lightweight medium-load applications in automobiles. The performance of bio additives can be improved for lightweight applications by incorporating the improved multi-response outcomes of fibers and surface treatments.

References

1. J.J.G. Sekaran, S. Duraithilagar, F.T. Josh, G. Kalusuraman, V.P. Srinivasan, and R. Karuppasamy, AIP Conference Proceedings. 2861[1] (2023) 04005.
2. N. Kumar, A. Singh, K. Debnath, and N. Kumar, Emerging Mater. Res. 9[1] (2020) 1-9.
3. A. Megalingam, M. Kumar, B. Sriram, K.Jeevanantham, and P. Ram Vishnu, Mater. Today Proc. 45 (2021) 723-728.
4. A.H. Elango, K.V. Kumar, T.G. Loganathan, R.K. Priya, S. Shobana, M. Balasubramanian, and J. Dharmaraja, J. Nat. Fibers. 19[13] (2022) 4949-4963.
5. G. Ram, T.V. Arjunan, K. Vinoth Kumar, and T.G. Loganathan, Waste Biomass Valorization. 16[2] (2025) 655-668.
6. G. Ram, T.V. Arjunan, T.G. Loganathan, I. Suyambulingam, and S. Siengchin, Biomass Convers Biorefin. 15[8] (2024) 11523-11535.
7. T. Raja, Y. Devarajan, and S. Thanappan, Sci. Rep. 13[1] (2023) 16291.
8. R. Ramkumar, K. Saranya, P. Saravanan, K.S. Perumal, P. Ramshankar, V. Yamunadevi, and P. Ganeshan, Mater. Today Proc. 51 (2022) 1096-1098.
9. T. Raja, D. Yuvarajan, S. Ali, G. Dhanraj, and N. Kaliappan, Sci. Rep. 14[1] (2024) 8374.
10. H.S. Sachin, K. Krishnaveni, K. Karthick, K. Chinnarasu, H.V.P. Prasad, A. Tonk, and S. Mayakannan, J. Environ. Nanotechnol. 13[4] (2024) 92-101.
11. V. Mohanavel, S. Suresh Kumar, J. Vairamuthu, P. Ganeshan, and B. NagarajaGanesh, J. Nat. Fibers. 19[13] (2022) 5258-5270.
12. S. Omprakasam, P. Vishnu, B.M. Ishanna, S. Abinaya Sree, and R. Divya Rani, Mater Lett. 380 (2025) 137750.
13. M. Elango, V. Naveen Krishna, A. Annamalai, and P. Harish, Lecture Notes in Mechanical Engineering. (2022) 491-501.
14. M. Sriariyanun, P. Baranitharan, S. Venkatesh, K. Rajeshkumar, and V. Kavimani, J Mater Cycles Waste Manag. 27[2] (2025) 880-897.
15. T. Singh, A. Aherwar, L. Ranakoti, P. Bhandari, V. Singh, and L. Lendvai, Sustainability. 15[11] (2023) 8880.
16. Y. Kandemir, T. Varol, and M. Aslan, Gümüşhane Üniversitesi Fen Bilimleri Dergisi. 13[4] (2023) 911-926.
17. A. Mitra, Res J of Text. Apparel. 28[2] (2024) 299-316.
18. M. Ponnuswamy, T.P. Sathishkumar, M. Selvaraju, and V.P. Sundramurthy, Arab. J. Sci. Eng. 49[11] (2024) 15733-15748.
19. R.K. Gupta, S. Mayakannan, S. Vijayaraghavalu, M.M. Poornima, S. Nanthakumar, and N.A. Bhaskaran, J. Environ. Nanotechnol. 13[4] (2024) 358-376.
20. N. Kumar, A. Singh, and K. Debnath, Mat. Test. 62[9] (2020) 937-942.

21. M. Azeem, S. Asim, A. Raza, H. Rasul, M. Ali, B. Khalid, R. Shukat, and A. Diantom, Cogent Food Agric. 10[1] (2024) 2396952.
22. S. Mohd Izwan, S.M. Sapuan, M.Y.M. Zuhri, and A.R. Mohamed, J. Mater. Res. Technol. 9[3] (2020) 5805-5814.
23. A.A.Mahamat, N. Leklou, I.I. Obianyo, P. Poullain, T.T. Stanislas, O. Ayeni, N.L. Bih, and H. Savastano Jr, J. Build. Eng. 62 (2022) 105411.
24. R. Gowrishankar, P.M. Sithar Selvam, K.S. Narayana, T. Raja, R. Gokul, and S. Mayakannan, J. Environ. Nanotechnol. 14[1] (2025) 306-322.
25. S. Wankhede, P. Pesode, S. Gaikwad, S. Pawar, and A. Chipade, Mater. Sci. Forum, 1081 (2023) 41-48.
26. D.T. Birkocak, E. Acar, A.Ç. Bakadur, B. Ütebay, and A. Özdağoğlu, Fibers Polym. 24[7] (2023) 2595-2608.
27. V.S. Chandrika, A. Anamika, C. Jeeva, B. Perumal, S.S. Kumar, J.F. Roseline, and I.K. Raghavan, Adv. Mater. Sci. Eng. 2022[1] (2022) 3035169.
28. V. Kavimani, B. Paramasivam, R. Sasikumar, and S. Venkatesh, Multiscale Multidiscip. Model. Exp. Des. 7[3] (2024) 1721-1736.
29. T. Singh, G.da Silva Gehlen, V. Singh, N.F. Ferreira, L.Y. de Barros, G. Lasch, J.C. Polett, S. Ali, and P.D. Neis, Results Eng. 22 (2024) 102030.
30. T. Raja, V. Mohanavel, S. Kannan, S. Parikh, D. Paul, P. Velmurugan, A. Chinnathambi, S.A. Alharbi, and S. Sivakumar, Heliyon. 10[8] (2024) e29818.
31. M. Sivaperumal, R. Thirumalai, S. Kannan, and Yarrapragada K S S Rao, J. Ceram. Process. Res. 23[3] (2022) 404-408.
32. K.M. Senthil Kumar, Thirumalai Ramanathan, Seenivasan Murugesan, and Venugopal Thangamuthu, J. Ceram. Process. Res. 22[6] (2021) 731-738.